MISR BAND-TO-BAND REGISTRATION

Jia Zong, Michael M. Smyth, and Veljko M. Jovanovic
Jet Propulsion 1 aboratory
Mail Stop 169-315
4800 Oak Grove Drive
Pasadena, CA 91109 USA

ABSTRACT

During the standard gee)-rcclificaliml processing of the M ISR imagery, all four spectral bands belonging to each of the nine M ISR cameras are required to be geolocated and co-registered automatically with about one pixel accuracy. Two steps of processing arc designed to accomplish Ibis goal: I) a complex multi-camera geolocation and co-registration of the red spectral band data for all nine cameras, and **2)** the co-registration of the other three spectral bands of M ISR imagery of each camera using their relationship with the already geolocated red band image.ry. This paper addresses the second processing. The geometry of the satellite orbit, the ellipsoid rotating earth, and the separation of the view angles between different spectral bands arc combined in a mathematical model which describes the band-to-band line and sample parallaxes. The sensitivity study of this model to numerous error sources, such as variations in the orbit and earth radius, orbit perturbation, and navigation errors, leads to a practical polynomial band-to-band transform solution, and the decision on the usage of either static or dynamic band-to-band transform as well as the application range of (he. transform.

Key Words: Geolocation, co-registrat ion, orbit perturbation, navigation error, image parallax, transform

1. INTRODUCTION

The Multi-angle Imaging SpectroRadiometor (MIS]<) instrument for the Earth Observing System (EOS) is to be launched in mid of 1998 aboard the EOS AM-1 satellite [Diner, 1991]. Its purpose is to study the ecology and climate of the earth through the acquisition of systematic, global multi-angle imagery in reflecting sunlight. The instrument consists of nine pushbroom cameras pointing at discrete view angles (one nadir, four forward and four aftward, at angles of 0°, ± 26.1 0, ± 45.6°, ± 60.0°, ± 70.50, designated as An for nadir, Af, Bf, Cf, Df for forward set and A a, Ba, Ca, 1 Da for aftward set of cameras). 1 ach camera is equipped with four spectral bands centered at 440, 550, 670, and 860 nm. During the first level standard processing of raw instrument imagery into science data, the 36 channels of **h41S1{** imagery are required to be geolocated and co-registered automatically with about onc pixel accuracy. The geolocated and co-registered multi-band imagery on the Space-Oblicluc Mercator (SOM) map projection will then be used in the subsequent level two geophysical parameter retrievals, such as aerosol optical depth and scattering properties, cloud classification, and albedos etc. As the output of this gco-rectification processing, a parameter called surface terrain projected radiance, as the part of the Georectified Radiance Products (GRP) family, will be derived. The surface terrain projected radiance is rcfcrc.need to the surface defined by the datum of WGS84 ellipsoid including 1)1 :Mover land and inland waler.

in order to meet the geolocation and co-registr alien accuracy requirement for all the 36 channels, a complex multi-camera geolocation and co-registration process utilizing the red spectral band data from all nine cameras is performed first [Jovanovic, 1996]. During this processing, image matching is performed between the input MISR imagery and the so-called MISR Reference Orbiting Imagery (ROI) for each camera in order to remove the distortions introduced by the topography and the relative static errors in the reported spacecraft ephemeris and attitude data during the imaging. The ROI for each camera (red band only) were set up during the posi-launch geometric calibration processing, from which a precise 1 inkage between the topographic surface and the cali brat ing MISR ROI are provided through the building of an ancillary data set called Projection Parameter data (1'1'). As a result of this first step of processing, wc have a direct mapping between the. surface terrain over the SOM map grid and the new M ISR red spectral band imagery for all nine. cameras. The next step is to provide a linkage further connecting to the other three spectral bands of cacb camera as shown in Figure 1, which is the subject of this paper.

The MISR band-lo-bard registration algorithm is designed to remove the band-to-band image parallaxes

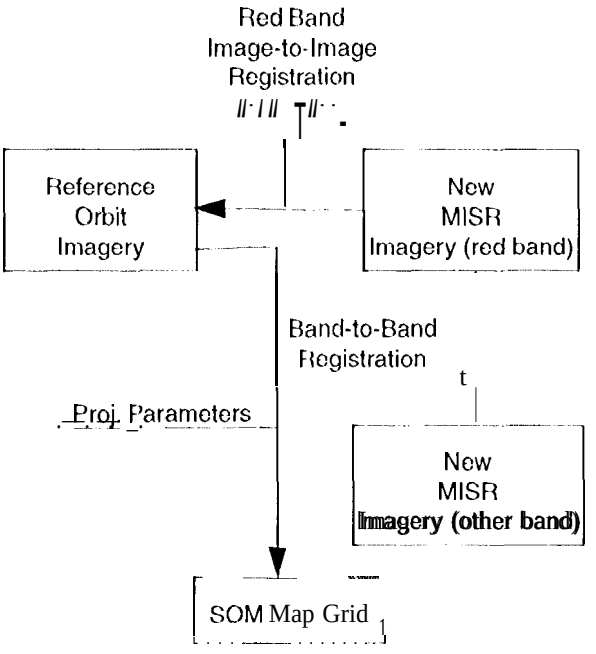

Figure 1: Georect ification Overview

between d ifferent spectral bands of the same camera caused by the separation of the bands on the camera focal plane. The underlying principles of the algorithm are the geometry of the camera structure and orbiting of the spacecraft over the earth. The mathematical model of these relations is simplified according the influence of various factors in order to provide a fast and accurate on-line registration. The main topics of this paper include the band-to-band relat ionship, the corresponding mathemat ical model, the error analysis of the model, and the algorithm implementation and test results.

2. MISR BAND-TO-BAND IMAGE PARALLAX

The MISR instrument has nine push-broom came]-as pointing toward different view angles. la order to provide imagery in four spectral band, each camera uses four Charge-Coupled Device (CCD) line arrays in a single focal plane. The line array consist of 1504 photoactive pixels plus 16 light- shielded pi xels per array, each 21µm x 18 pm. 1 Each line array is filtered to provide onc of the four MISR spectral bands, shaped nominally Gaussian and centered at 443, 555, 670, and 865nm. The cross-track instantaneous field of view (IFOV) and sample spacing of each pixel arc 275 m for all the off-nadir cameras and 250 m for the nadir camera. The along-track IFOV depends on view angle, ranging from 250 m in the nadir to 707 m at the most oblique angle though sampling spat.c is always 275 m in all cameras.

Because of the. physical displacement of the four line arrays within the focal plane of each camera, there is a displacement in the earth view at the four spectral bands. Figure 2 illustrates the spatial displacement the four CCD line arrays relative to detector coordinate system. Nominally, band number 3 is locate.d in the y-z plane, and the sepa-I-alien between bands is equal to 160 pm. The image displacement of the same surface. feature resulted from band to band due to this kind of camera design is characterized by two value.s called line-parallax and sample-parallax. Line-parallax is the direct result of the time difference between imaging a ground point by two different hands. Sample-parallax represents difference in the sample coordinates (i.e., in the direction across the band) of the same ground point projected to the imagery corresponding to the different bands.

In order to compute magnitude of both line and sample pat-al laxes from band to band, a simulated navigation

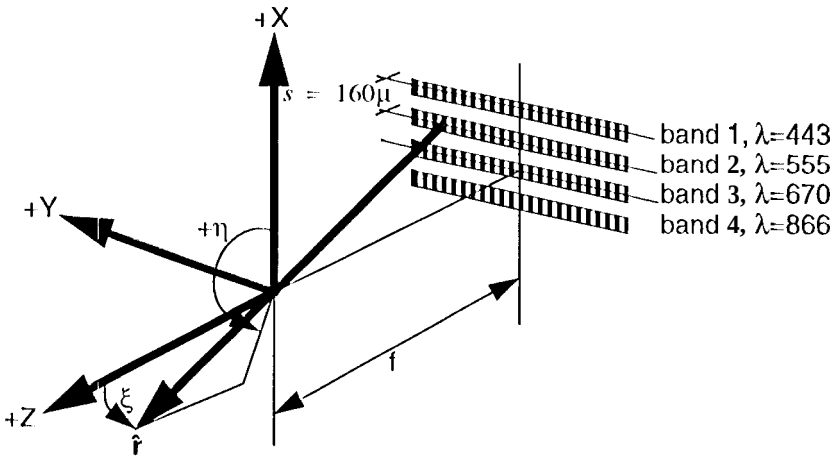

Figure 2: Four line detectors (i.e., bands) in a single focal plane

data, nominal geometry of the cameras, and surface topography of the earth represented by a 1)1 :M arc used. At first, a forward projection of a scan 1 ine of rays corresponding to the reference band, band 3, is performed in order to find ground points seen at known line and sample coordinates in the spectral band 3 imagery. Then, a backward projection for a band of interest is performed in order to find line and sample coordinates of the same ground points seen by the imagery representing the band of interest (e.g. band 1). Differences between the known line and sample coordinates of band 3 and those of band 1 for one scan line of the reference band are plotted in Figure 3 and Figure 4. Both line

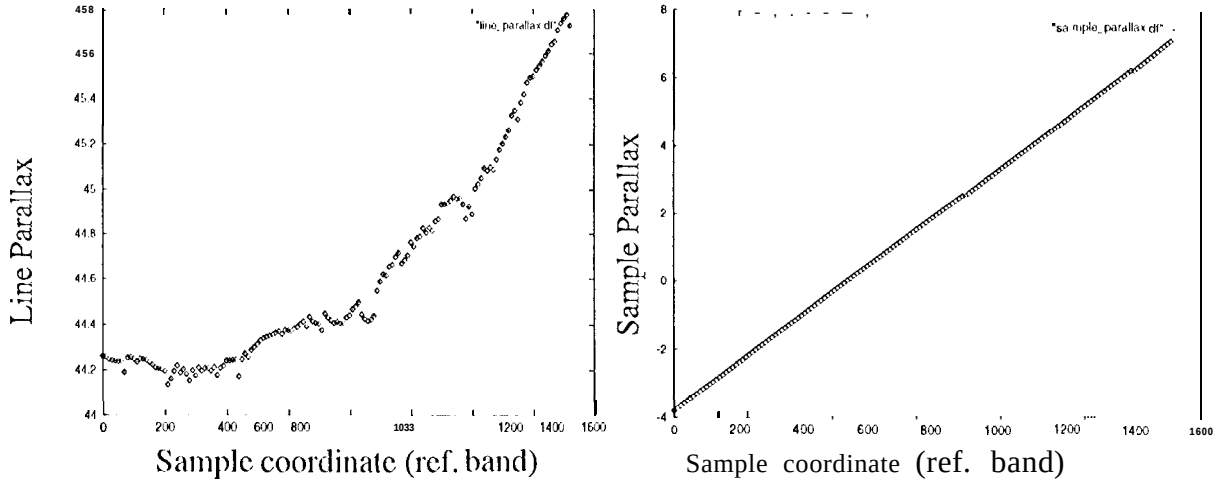

Figure 3: Line and sample parallaxes of Df camera

and sample, parallaxes are plotted against sample coordinates of the reference bad. The Df camera designates the most oblique forward camera and the Aa camera designates the least oblique aftward camera. As seen from these two figures, line parallax is mostly a function of the camera type, the geometry Or the rotating ellipsoid earth, and tbc fluc-

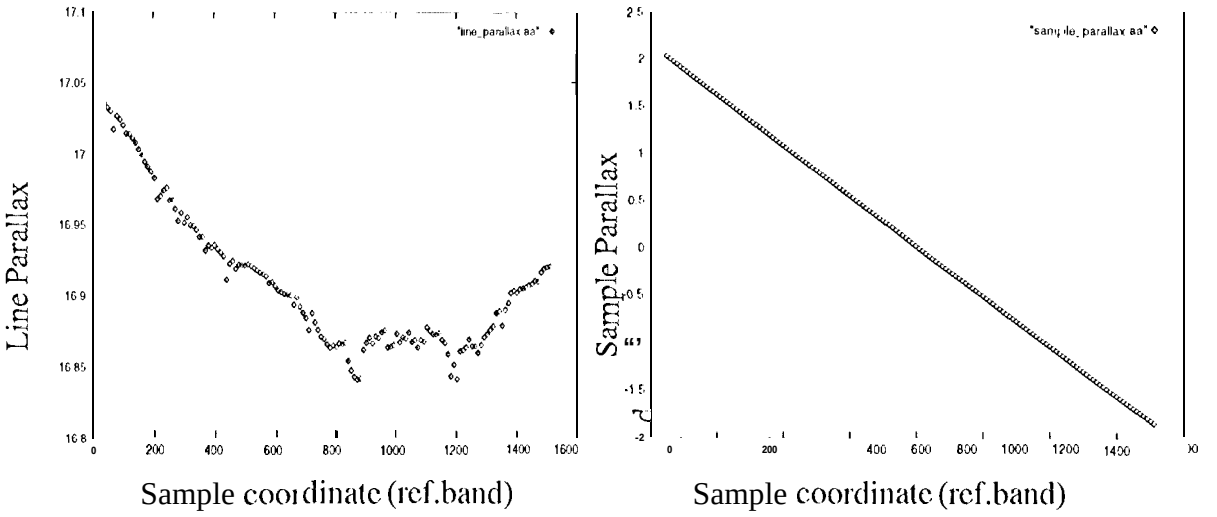

Figure 4: Line am] sample parallaxes of Aa camera

tuation of the topography. Similarly, the same factors influence the sample parallax. The goal of band-to-band registration is to remove these parallaxes with a minimum usc of data storage and processing lime while still satisfying geolocation and co-registration requirements.

3. MATHEMATICAL MODEL OF IMAGE PARALLAX

3.1. Line Parallax

Assuming a spherical Earth, a circular orbit, and no attitude change during the time corresponding to the line parallax (the effects of the terms that are ignored will be discussed later), the line parallax from band of interest to the reference band is the result of the geometry illustrated by Figure 5. From this figure, the following relation can be established:

$$\Delta\alpha = \beta_r - \beta - \operatorname{asin}\left(\left(\frac{R_s}{R_e + H}\right)\sin\beta\right) + \operatorname{asin}\left(\left(\frac{R_{sr}}{R_e + H}\right)\sin\beta_r\right) \tag{1}$$

Line parallax A/ can be related to the angle $\Delta\alpha$ through Kepler's modified equation[Herrick, 1971] as:

$$\Delta l = \sqrt{\frac{a^3}{\mu}}\left(\Delta\alpha - \left(1 - \frac{R_s}{a}\right)(\sin\Delta\alpha) + \frac{(r \cdot v)}{\sqrt{\mu a}}(1 - \cos\Delta\alpha)\right) \tag{2}$$

where a = orbit semi major axis, r and v are spacecraft radius and velocity vectors, μ = Earth gravitational-mass constant, and t_l = time. interval between recorded lines. With the assumption that orbit is circular, Equation (2) is simply,

$$\Delta l = C_{11}\Delta\alpha + Error1 \tag{3}$$

where C_{11} is constant. Equation (3) and (1) can be combined and expanded as Taylor series with H, the only variable varies significantly during the time from band to band,

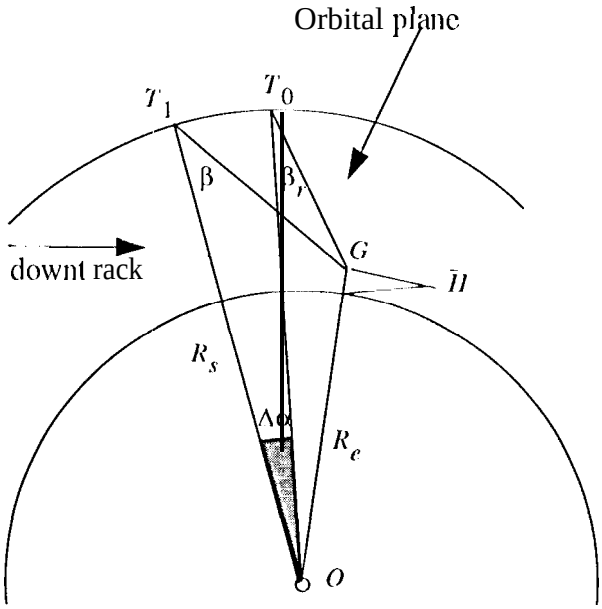

R_s - orbit radius

R_e - Earth radius

$\bar{H}$ - ground point height projected to the orbital plane

β_r - view angle reference band 3

β - view angle band of interest

Figure 5: Simplified geometry illustrating line parallax

$$\Delta l = C_{21} + C_{22}\bar{H} + \ldots Error2 \quad (4)$$

The coefficients C_{21} and C_{22} can be estimated with the known line parallax of selected control points through a least-squam fitting. The variable H in Equation (4), which represents the ground height on the orbital plane, must be converted from the true ground height of the. image point onto the orbital plane according to camera pointing. Figure 6 ill ustrates geometry used to compute the projected height given the image sample number y and height II, from

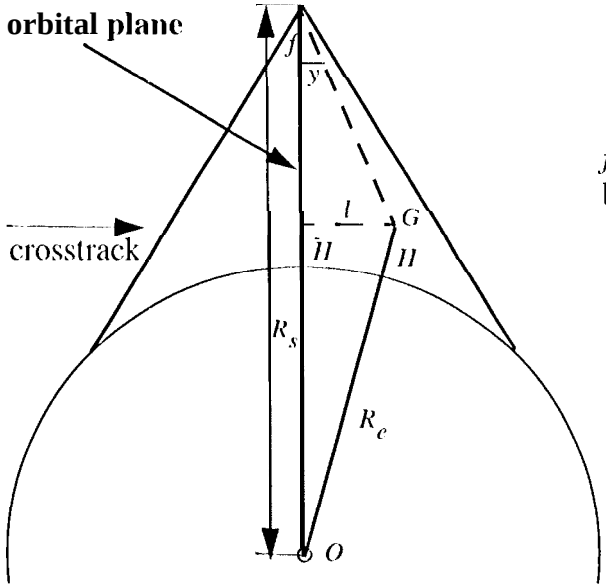

y = sample $\#$

C_4, = '7s2 for nadir camera

f as focal length (reference band)

Figure 6: Height Projection onto orbital plane

which two relations about l are formed:

$$l = \frac{y}{f}(R_s - R_e - H), \tag{5}$$

$$l^2 = (R_e + H)^2 - (R_e + \bar{H})^2 \tag{6}$$

Combine 1 Equation **(5)** and (6) and solve the quadratic equation (smaller of the two possible solutions), $\bar{H}$ is equal to:

$$\bar{H} = \frac{\left\{\frac{y^2}{f^2}R_s - \sqrt{\frac{y^2}{f^2}(R_e + H + R_s)^2 - (R_e + H)}\right\}}{\frac{y^2}{f^2} - 1} - h'_c \tag{7}$$

Because some of the relations (e.g., $y < sample$) due to the roll and pitch angles are not taken into account analytically. Equation (7) is expanded to tbc Taylor series with variables height, image sample coordinate s, and the nadir sample location C_{41},

$$\bar{H} = C_{31} + C_{32}H + C_{33}(s - C_{41}) + C_{34}(s - C_{41})^2 + \ldots Error3 \tag{8}$$

In summary, tbc line band-to-band parallax can be computed with tbc following transform equation:

$$\Delta l = C_{21} + C_{22}H + C_{23}(s - C_{41}) + C_{24}(s - C_{41})^2 + \ldots Error4 \tag{9}$$

3.2. **Sample parallax**

The sample parallax is result of: 1) scaling between reference band and band of interest due to different IFOV, 2) shift due to small roll angle variation, 3) shift due to the Earth rotation. These effects can be modeled as the linear scaling plus shift,

$$s_{new} = D_{11} + D_{12}s_{ref} \tag{10}$$

The coefficients D_{11}, and D_{12} can be pre-estimated through a least-square fitting as well.

4. ERROR ANALYSIS OF MODEL

In order to determine the transform coefficients and their application range, and to estimate the error magnitude introduced during the model simplification, an error analysis was conducted.

4.1. Error Analysis of Line Parallax

The following factors contribute to the error in the line parallax determination: 1) error in the projected height $\bar{H}$; 2) variation of the earth radius R_e; 3) variation of the orbit radius R_s; 4) fractional orbit radius variation from band to band ΔR_s; 5) error in the spacecraft pitch attitude β; and 6) fractional spacecraft pitch attitude variation from band to band $\Delta\beta$. The effects of these errors are estimated by calculating the final error in line parallax using

Equations (1), (2), and *(7).* The results are summarized in Table land the following conclusion is made accordingly:

'J'able 1: Sensitivity of the I .ine Parallax Model for Spectral Band 1

Error for Camera	εH = 1000.0 m	εR_c = 700.0 m	εR_s = 160.0 m	ΔR_s = 0.02 m	$\varepsilon\beta$ = 150 arc-sec	$\varepsilon\Delta\beta_s$ = 4 arcsec
Af (line)	0.028	0.038	0.009	**0.000**	**0.013**	0.061
Df (line)	0.146	0.204	0.045	**0.000"**	**0.252**	**0.340**

- Errors in surface elevation or DEM is negligible.
- For WGS84 ellipsoid, **700 m** changes in the earth radius R_c corresponds to 3° latitude change or 1200 MISR orbit lines. The earth radius variation limits the application range of a set of band-to-band line transform.
- Both the orbit variation and the fractional orbit variation factors are negligible according to the TOS-AM spacecraft orbiting specification.
- The fact that attitude angles may perturbed from the spacecraft specification limits tbc capability of pre-estimating the band-to-band transform coefficients with a nominal orbit specification instead of dynamically calculating on line.
- The 4 arcsec is a conservative error estimate of altitude error during the maximum time difference between bands (for the most oblique D cameras). This error corresponds to the un-corrected navigation error between band of interest and the reference band, which is a major source to the band-to-band registration error.

4.2. Error Analysis of Sample Parallax

The three factors affect the sample registration are indicated in §3.2. The first factor is a constant. The behavior of factional roll angle variation during the time pet iod from band to band is similar to that of pitch angle. The influence of the earth rotation depends on the location of the orbit. Its impact can be illustrated by assuming that a sample displacement corre sponds to a change in the longitude direction, as $Ad = R_\phi \Delta\lambda_b = R_e \omega \Delta t_b \cos\phi$, where R_e is the earth radius, R_ϕ is the earth radius at latitude ϕ relative to the earth rotating axis, Ad is the earth rotation distance at this latitude during the time period Δt_b between two bands were imaged. For the most oblique D cameras, Δt_b = 1.9 second. The change, on this rotation distance Δd due to a latitude change of $\Delta\phi$ is:

$$\Delta s = \frac{\partial}{\partial\phi}(\Delta d)\Delta\phi = -R_e \omega \Delta t_b \sin\phi \Delta\phi \qquad (11)$$

Equation (11) relates the scaling of band-to-band sample parallax As to an orbit traveling segment $\Delta\phi$. It is obvious this scaling factor varies at different latitude due to the earth rotation. To determine the application range of a set of sample band-to-band transform coefficients, the orbit lines Δl corresponds to tbc same segment of swath $\Delta\phi$ can be directly related to Δs as:

$$\Delta l = 7352 \Delta s \qquad (12)$$

4.3. Conclusion of Error Analysis

The following conclusion arc made according to the error analysis of both line and sample band-to-band registration mode]:

- The application range of tbc sample transform should be less than 2000 orbit lines mainly clue to the earth rotation.
- The application range of the line transform should be less than 1000 orbit lines mainly due 10 the earth radius variation.
- The transform coefficients can be determined either once. at the pos(-launch MISR geometric calibration phase

(using nominal view angles), or dynamically during the standard processing of MISR imagery data.

5. ALGORITHM IMPLEMENTATION AN1) TEST RESULT

I bring a recent Beta version of standard processing, the dynamic determinat ion of band to band coefficients was implemented and tested.

'1'here is some uncertaint y about what the stability of the EOS-AM1 platform will be. The predicted behavior is substantially better than the requirements. For purposes of band-to-band, the error analysis in §4.1 and §4.2 strews that the short term stability of the attitude is more critical. Table 2 shows both the predicted and the required stability

"I'able 2: MISR Jitter/Stability

Time Scale (seconds)	Maximum Perturbation (arcseconds, 3σ)		
	Roll	Pitch	Yaw
0.1	0.8	1.7	1.5
1.0	1.9	2.6	2.2
1.0 Requirement	8.0	8.0	8.0
1.8	2.2	3.0	2.6
6.0	3.3	5.2	4.7
9.0	4.2	6.5	6.1
12.5	4.6	7.1	6.4
420.0	9.7	13.1	10.6
420.0 Requirement	20,0	2.0.0	20.0
480.0	9.9	13.9	10.6

of the EOS-AM1 platform

To test the band -to- band algorithm, simulated MISR imagery, reference orbit imagery (ROI), and projection parameters (PP), was created. The simulated MISR imagery was based on Landsat Thematic Mapper ('I"M) data, along with a registered DEM. A Universal Transverse Mercator (UTM) plate of an area of central Mexico with a map scale of 28.5 m was used. The simulation process is described in [Lewicki, 1994]. For this test, the simulation was performed once. for a simulated orbit with predicted stability, and once. for an orbit that only meets stability requirements.

1 Each set of band-to-band transform coefficients were determined using a set of well distributed control points over a segment of orbit as described above. The transform was used to resample the simulated MISR imagery onto the SOM map grid. The band-to-band error for the 1)]: (most aftward looking camera) was 0.30 pixels (95% confidence level) in the along track direction for the predicted platform stability, and 0.68 pixels (95% confidence level) in the along track direction for the required stability.

The band-to-band error was also measured for the AN (nadir looking camera), but the resulting error was smaller than our test procedure could measure (less than 0.08 pixels).

6. SUMMARY

By using the geometry of the MISR camel a, we have developed a band-to-band transform that allows us to co-register the four band of tbc MISR instrument. This transform has been implemented, and shown to meet our co-registration requirements and wet-k well in practice.

7. ACKNOWLEDGMENTS

The authors gratefully acknowledge the efforts of the MISR Science Data System Team: Earl G. Hansen, Scott A. Lewicki, Kyle C. Miller, and Alec B. Shaner. This research is being carried out at the Jet propulsion laboratory, California Institute of Technology, under contract with the National Aeronautics and Space Administration.

8. REFERENCES

Diner, D. J., Bruegge, C. J., Martonchick, J. V., Bothwell, G. W., Danielson, E. D., Floyd, E. L., Ford, V. G., Hovland, L. 1;., Jones, K. 1... and White, M. 1... A Multiangle Imaging SpectroRadiometer for Terrestrial Remote Sensing from the Earth Observing System, International Journal of Imaging Systems and Tech, 1991

Herrick, S., Astrodynamics, Van Nostrand Reinhold, New York, 1971

Jovanovic, V. M., Smyth, M. M., and Zong, J., Autonomous and Continuous Georectification of Multi-angle Imaging Spectro-Radiometer (MISR) Imagery, ISPRS Int. Arch. of Photogrammetry, vol. XVIII, Commission III, Vienna, 1996

Lewicki, S. A., Smyth, M. M., Jovanovic, V. M., and Hansen, E. G., A Simulation of EOS MISR Data and Geometric Processing for the Prototyping of tbc MI&l Ground Data System, IGARSS, vol 11 I, Pasadena, CA 1994